THE SPATIAL DISTRIBUTION AND TIME EVOLUTION OF IMPACT-GENERATED MAGNETIC FIELDS. D. A. Crawford and P. H. Schultz, Dept. of Geological Sciences, Brown University, Providence, RI 02912.

The production of magnetic fields has been revealed by laboratory hypervelocity impacts in easily vaporized targets performed at the NASA Ames Vertical Gun Range[1,2]. As quantified by pressure measurements, high frame-rate photography and electrostatic probes, these impacts, tend to produce large quantities of slightly ionized vapor, which we refer to as impact-generated plasma[3-6]. Nonaligned electron density and temperature gradients within this plasma may lead to the production of the observed magnetic fields[7]. Past experiments were limited to measuring a single component of the impact-generated magnetic field at only a few locations about the developing impact crater and consequently gave little information about the field production mechanism. To understand this mechanism, we are extending our techniques to map the three components of the magnetic field both in space and time. By conducting many otherwise identical experiments with arrayed magnetic detectors we have produced a preliminary three-dimensional picture of impact-generated magnetic fields as they develop through time.

The magnetic detector array consists of fifteen overlapping search coils. Each coil, consisting of several hundred turns of 30 gauge copper magnet wire wound helically on an 8 cm plastic form, measures a single component of the magnetic field. The position of the search coils (x,y,z) is recorded with the origin at the point of impact, where +z measures the height (in cm) above the target surface, +y the distance uprange of the impact point and +x the distance away from the projectile line-of-flight in a right-handed sense. Fig. 1 is a time sequence of the magnetic field observed at τ = 1200, 1800 and 2400 R_p/V_p (~0.33, 0.50 and 0.66 ms respectively) after the first contact of a 0.32 cm Fe projectile impacting a powdered dolomite target at a mean velocity of 5.75 km/s. The field observed within the target varies considerably with time but is predominantly horizontal. In the first time step (Fig. 1a), the field is nearly toroidal - consistent with near vertical electric currents in the plasma cloud. This suggests that the plasma is contained and redirected by the developing crater. The strong, homogeneous field in the second time step (Fig. 1b) is consistent with a large current system in the more extensive plasma cloud. In the final time step (Fig. 1c), the field is beginning to decay and the signals are consistent with local currents in the plasma that remains near the crater.

A relatively low signal-to-noise ratio results from two factors: 1) the impact-generated magnetic field far from the impact point is contaminated by interactions between the ambient field and the expanding plasma; the external (ambient) magnetic field has large gradients throughout the impact region making it difficult to entirely remove with cancellation techniques. Previously, this was not a problem as the impact-generated magnetic fields were observed in a limited area about the impact point. 2) the impact-generated magnetic field, though reproducible, varies enough from shot to shot to introduce a noise term when data sets are combined in this way. In future experiments, a passive magnetic shield should significantly reduce noise from the first factor while averaging many data sets should reduce noise from the second factor.

In a parallel set of experiments, the spatial extent and time evolution of impact-generated plasma is being derived with the use of electrostatic probes. Eventually, we want to determine the early-time projectile/target interaction that yields impact-generated plasma, to understand the production and remanence mechanisms of impact-generated magnetic fields and to find the scaling laws that will allow us to extend these observations to planetary scale.

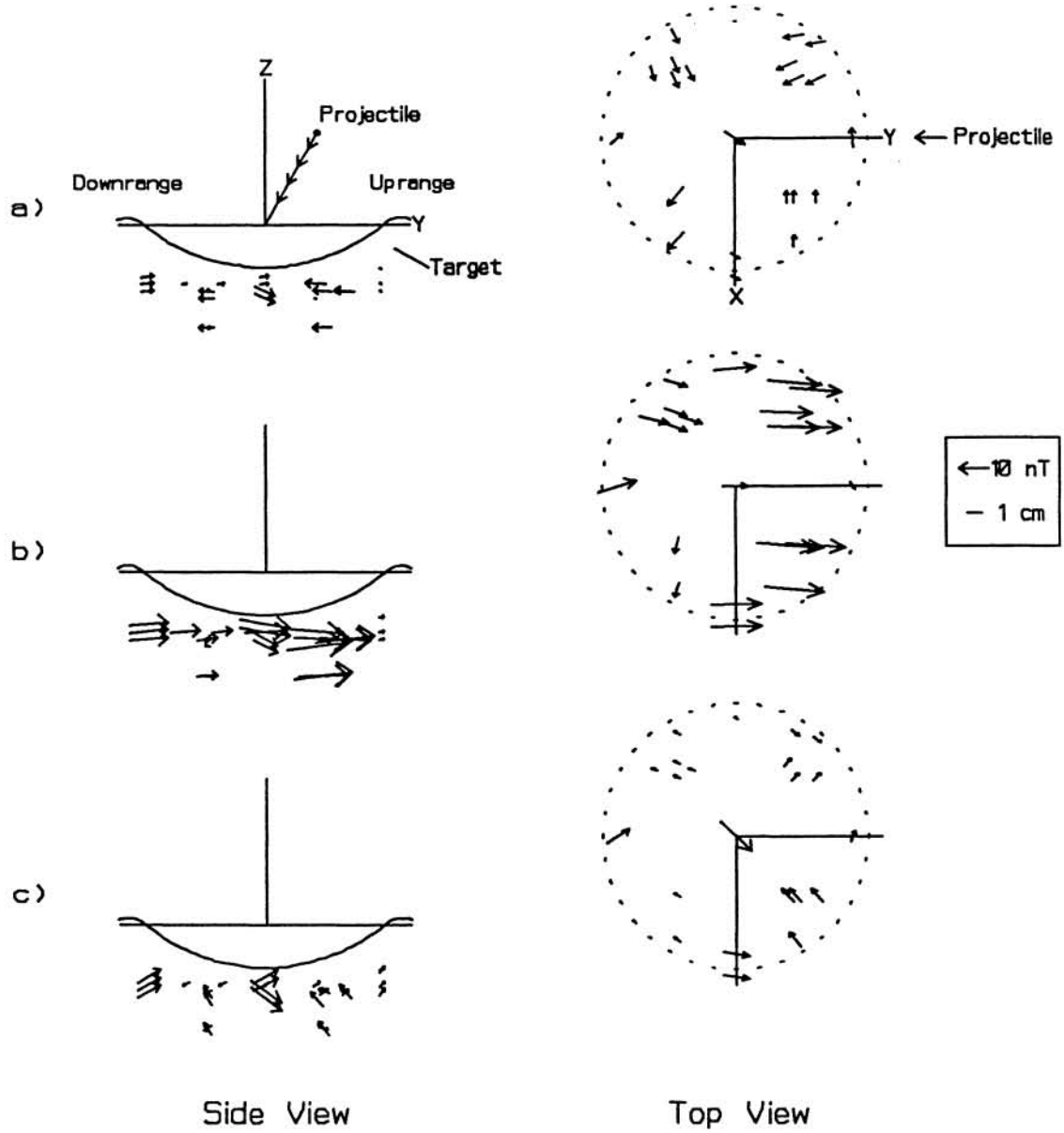

Fig. 1 Time sequence of the observed magnetic field at: a) $\tau = 1200\ R_p/V_p$ (~0.33 ms), b) $\tau = 1800\ R_p/V_p$ (~0.50 ms), and c) $\tau = 2400\ R_p/V_p$ (~0.66 ms) after the first contact of a 0.32 cm Fe projectile impacting into a powdered dolomite target at a mean velocity of 5.75 km/s. This plot is a compilation of data from three nearly identical impacts at 5.52, 5.83 and 5.90 km/s. The projectile trajectory prior to impact was in the Y-Z plane, 60° from horizontal. First contact occurred at the origin. The final crater extent is shown in the Side View as the solid profile and in the Top View as the dashed circle.

[1] Crawford, D.A. and Schultz, P.H., Nature 336, 50-52 (1988). [2] Crawford, D.A. and Schultz, P.H., Lunar Planet. Sci. 20th, 197-198 (1989). [3] Crawford, D.A. and Schultz, P.H., Lunar Planet. Sci. 21st, 242-243 (1990). [4] Crawford, D.A. and Schultz, P.H., J. Geophys. Res. (in revision). [5] Schultz, P.H., Lunar Planet. Sci. 19th, 1039-1040 (1988). [6] Schultz, P.H. and Gault, D.E., Geo. Soc. Amer. Bull. 247, (in press). [7] Srnka, L.J., Proc. Lunar Sci. Conf. 8th, 893-895 (1977).